Catena 140 (2016) 205–216

Contents lists available at ScienceDirect

Catena

journal homepage: www.elsevier.com/locate/catena

Control factors of the spatial distribution of arsenic and other associated elements in loess soils and waters of the southern Pampa (Argentina)

Silvana Letisia Díaz [a], Martín Eduardo Espósito [a], María del Carmen Blanco [a,*], Nilda Mabel Amiotti [a,b], Erica Susana Schmidt [a], Mario Eduardo Sequeira [b,e], Juan Darío Paoloni [d], Hugo Benjamín Nicolli [c,d]

[a] Depto. de Agronomía, Universidad Nacional del Sur (UNS), San Andrés 850, 8000 Bahía Blanca, Argentina
[b] Centro de Recursos Naturales Renovables de la Zona Semiárida (CERZOS), E-1 CCT BB, Camino de la Carrindanga, km 7, 8000 Bahía Blanca, Argentina
[c] Instituto de Geoquímica (INGEOQUI), San Miguel, Prov. de Buenos Aires, Argentina
[d] Consejo Nacional de Investigaciones Científicas y Técnicas (CONICET), Centro de Investigaciones San Miguel, San Miguel, Prov. de Buenos Aires, Argentina
[e] Depto. de Ingeniería, Universidad Nacional del Sur (UNS), Av. Allem 1253, 8000, Argentina

ARTICLE INFO

Article history:
Received 27 October 2014
Received in revised form 30 December 2015
Accepted 14 January 2016
Available online xxxx

Keywords:
Loess sediments and soils
As geoavailability
Hydrochemistry
Water quality

ABSTRACT

Surface and groundwaters of El Divisorio brook (Argentina) have excessive As (WHO, USEPA, CAA: >10 μg L^{-1}). The rural population is at risk of arsenicism because groundwater is the only source of water for human consumption. We analyse geoavailability of As and other associated elements (Ba, Br, Co, Cr, Fe and Na) in the solid phase (INAA-Actlabs), determine the association between As and other elements in the mineral suite and in waters, quantify Fe oxides (Fe_{ox}; Mehra and Jackson) and interpret their relationship with As, total Fe (Fe_{total}) and Na in the solid phase applying Principal Components (PC) to understand factors and processes that rule their incorporation into groundwaters and to identify areas at risk of elevated As in waters. Intrabasin variability of total As content (range 5.80–20.70 mg kg^{-1}) with the highest amounts towards the discharge areas and a more irregular vertical distribution, particularly in the alluvial plain, reflects differences in As-bearer frequencies. Arsenic is slightly lower in the Bw horizons compared with the A and C horizons and it increases in the Bt horizon through clay illuviation. More than 90% of sodium-bicarbonated surface and groundwaters showed As >10 μg L^{-1} (range: 10 to 114 μg L^{-1}) with the highest levels in the middle–lower basin. The highest contributions to PC1 were Br (0.673), Co (0.868) and Na (−0.769); As (0.814) and Cr (0.686) were relevant to PC2 and Ba (0.501) and Fe (0.783) were relevant to PC3. In the upper basin, a greater amount of Na withheld in the solids promotes a less aggressive geochemical environment and prevents As from entering waters, thus yielding lower As levels in the aquifer compared with the middle–lower basin. Here, alkalinity (pH: 7 up to >9) promotes weathering and liberation of As from volcanic glass and other carriers, formation of As oxyanion species together with As desorption from charged clays and Al–Fe–Mn sesquioxides and concentration up to unacceptable levels in solution. Landform configuration, climate and pedoclimate, the residence time of water and the local hydrogeochemical variables (pH, competition with other ions, adsorption–desorption) control mobility and concentration of As in a dynamic equilibrium with the local chemistry. Evaporation (subhumid to semiarid climate) and oxyion competition reinforce As accumulation in the shallow aquifers.

1. Introduction

Geoavailability of As in the solid phase of loess and loess-derived soils and sediments and the subsequent incorporation into the aqueous phase of the Pampean aquifers, where it eventually reaches unacceptable concentrations, puts at risk the health of people who only use affected groundwaters as drinking water. These aspects transversally connect pedology, sedimentology, hydrology and medical geology with the aim of explaining the relationship between natural geological factors and the population's health as well as the geographical distribution of certain medical problems such as hydroarsenicism. Access to water is one of the decisive factors for global, regional and local development. The volume and quality of the water supply and its suitability for diverse uses is a challenge faced by most countries. The United Nations have declared the provision of potable water as a citizen's right, which, for a significant number of inhabitants of rural and periurban areas, is denied owing to the presence of natural contaminants that limit water suitability for human and cattle consumption as well as for developing

* Corresponding author.
E-mail addresses: silvanadiaz@criba.edu.ar (S.L. Díaz), mesposito@uns.edu.ar (M.E. Espósito), mcblanco@criba.edu.ar (M.C. Blanco), namiotti@criba.edu.ar (N.M. Amiotti), eschmidt@criba.edu.ar (E.S. Schmidt), sequeira@uns.edu.ar (M.E. Sequeira), jpaoloni@criba.edu.ar (J.D. Paoloni), hbnicolli@gmail.com (H.B. Nicolli).

http://dx.doi.org/10.1016/j.catena.2016.01.013
0341-8162/

irrigation projects (Bundschuh et al., 2008a). Particularly, As concentrations exceeding the provisional guide value (GV: 10 μg L^{-1}), which is accepted by the World Health Organization (WHO, 2008) and coincides with the maximum contaminant level (MCL) of the Environmental Protection Agency (USEPA, 2014) and the Código Alimentario Argentino (CAA; Argentinian Food Code, 1994), cause toxicity in surficial and groundwater resources. Regardless of their source, arsenic-contaminated waters (As >10 μg L^{-1}) harm human health and can be an important limitation due to their effects on agriculture and cattle production based on waters developed through sourcing with waters high in As and coexisting with other trace elements (F, V, B, etc.). According to the WHO, USEPA and CAA, acceptable concentrations of these elements in human drinking water are: As <10 μg L^{-1} and F <1500 μg L^{-1}. Moreover, in areas with a mean annual temperature close to 15 °C, the CAA sets 800 μg L^{-1} as the lowest recommended concentration of F in waters for human consumption. On the other hand, the CAA establishes a maximum value of 500 μg L^{-1} for B, which has been recently modified to 2400 μg L^{-1} (WHO, 2015). Currently, neither a guide value (WHO) nor a maximum contaminant level (USEPA, 2012) is considered for V.

In several worldwide regions, long-term consumption of high As waters has resulted in the development of Regional Endemic Chronic Hydroarsenicism (HACRE, for its Spanish acronym) and it may cause palmo-plantar keratodermia, diverse types of cancer, digestive system, liver and kidney lesions, cardiac, vascular and neurological disorders, among other symptoms (Besuschio et al., 1980; Hopenhayn-Rich et al., 1997, 1996). Generally, these symptoms become more frequent in populations with a high level of poverty, which solely in Ibero-America implies betwen 2 and 8 million people at potential risk (Bundschuh et al., 2008a, 2008b; Nicolli et al., 2012).

The areas affected by As in Argentina are larger than in India and Bangladesh; however, the genesis and source of As contamination are completely different (Chakraborti et al., 2010; Chatterjee and Mukherjee, 1999; Garnier et al., 2011; Mukherjee et al., 2009, 2008; Nicolli et al., 2012, 2008, 1997) and the problem in Argentina is much less investigated. In accord with Anawar et al. (2002) and Mc Arthur et al. (2001), elevated As in the aquifers of Bangladesh originates from reductive dissolution mechanisms in a geochemical environment with marked acidity associated with a great amount of sulphides and peat levels interspersed in the pedosedimentary column. Furthermore, the excessive As of the Pampean aquifers is related to its geoavailability in the pre-Quaternary loess sediments and loessic soils of aeolian origin and Holocene age containing volcanic glass as an important constituent that, with or without alluvial reworking, integrates the pedosedimentary sequences that host the phreatic aquifers (Blanco et al., 2006; Nicolli et al., 2012, 1997, 1989; Smedley and Kinniburgh, 2002).

Despite the high concentrations of As and other trace elements that eventually affect water quality, their contents in the loess solid phase, in general, and in volcanic glass, in particular, are generally normal or slightly higher than and analogous to those in the earth crust (2–6 ppm; Morrás et al., 2002; Rankama and Sahama, 1962). Besides its direct effect on public health, arsenotoxicity is attracting further attention due to the potential transference of As ion from soils and waters to crops and cattle, and its subsequent incorporation into the human food chain (Chatterjee et al., 2010; Xie and Naidu, 2006). The hydrochemistry of the so-called unsaturated zone (USZ), the interval of the stratigraphic column located between the topsoil and the phreatic level, is closely related, at least partially, to the mineralogical composition of the soils and sediments. Thus, the pedological participation regarding the source and the distribution of contaminant elements in the aquifers is relevant (Blanco et al., 2006).

In the southern Pampean region, the hydric resources of El Divisorio brook discharge into Paso de las Piedras dam, which is the only potable water reservoir for Bahía Blanca and Punta Alta cities (Buenos Aires province, Argentina). These urban nuclei together have a population of more than 400,000 inhabitants. In the adjacent rural areas, the water provision source for diverse uses is solely the phreatic aquifer, which in turn, usually has elevated As and other trace elements that may affect the health of the population devoid of tap water. The origin of arsenic toxicity is interpreted in terms of the soil and sediment geochemistry. Several authors have linked the high As in groundwaters of Pampean areas to the presence of volcanic glass and volcanic ash (Nicolli et al., 2012, 1997; Smedley and Kinniburgh, 2002) in the pedosedimentary sequences that host the phreatic aquifer. Although volcanic minerals and volcanic glass, particularly of the acid type, coexist in varying proportions in the mineral suite of loess and loess-derived sediments, interspersed volcanic ash layers were not identified in the sedimentary succession of the studied region.

The transference of As from soils and waters to cattle, crops and, later, to the food chain increases the potential risk of toxicity derived from daily human consumption of As-contaminated drinking waters. Our working hypothesis was that total As geoavailability in soils and sediments and its spatial distribution is controlled by the sedimentary dynamics of El Divisorio brook. Moreover, iron-oxidizing species control As levels transferred to waters while Na that regulates the pH is another factor that affects As availability and its transference to surface and groundwater resources.

The objectives of this work are: i) to analyse geoavailability of As and other associated elements (Ba, Br, Co, Cr, Fe and Na) in the solid phase of soils and sediments through which rainfall water circulates to feed the shallowest aquifer or which are in direct contact with the phreatic level, ii) to quantify Fe oxides (Fe_{ox}) and interpret their relationship with As, total Fe (Fe_{total}), and Na in the solid phase, iii) to perform multivariate statistical analyses in order to determine the association between As and the other elements present in the mineral suite of sediments and in the waters of El Divisorio basin, iv) to establish the interrelationship between the solid phase and water so as to understand the factors and processes that control those elements incorporation into groundwaters, v) to investigate the spatial distribution of As concentrations in groundwater in order to identify areas at risk by preferential accumulation of elevated As.

2. Materials and methods

The study area comprises the endorheic basin of El Divisorio brook situated in the southern portion of the Pampean plain, covering an area of approximately 400 km^2 (Fig. 1). This unit is part of the morphostructural domain of the Ventania hills system and dissects both the hilly piedmont and a sector of the Subventánica Occidental plain in the south of Buenos Aires province (Espósito et al., 2008; González Uriarte, 1984). In this region, the Ventania system is the only positive relief that behaves as a dispersion center of the surface and groundwater flows generated by rainfall (Paoloni et al., 1988). The main course of the basin is permanent, extends along 40 km, collects waters from the western slope of Sierra de Pillahuincó, and discharges into Paso de las Piedras dam (38° 25′ S and 61° 45′ W).

The regional climate is transitional between humid temperate and suhumid dry. The mean annual rainfall is 750 mm and the mean annual temperature reaches 14 °C (mean summer temperature: 20 °C; mean winter temperature: 8 °C). Freezing and occasional snow occurs when temperature is <0 °C (Paoloni et al., 1988). Pedoclimate is udic–thermic. Rainfall is regularly distributed in normal years and the dry season is limited. Towards the SW, the soil moisture regime is transitional to ustic with a marked seasonal distribution of rainfall. The dry season comprises the winter (June, July and August) and part of the summer, when evapotranspiration is considerably higher. However, despite the higher rainfall level in January, March and April, there is a critical water deficit during the summer due to a greater demand for evaporation.

Two toposequences (A and B) were selected respectively in the upper and in the middle–lower basin (Fig. 1). In each section, the soils associated with different landforms were described (Soil Survey Staff,

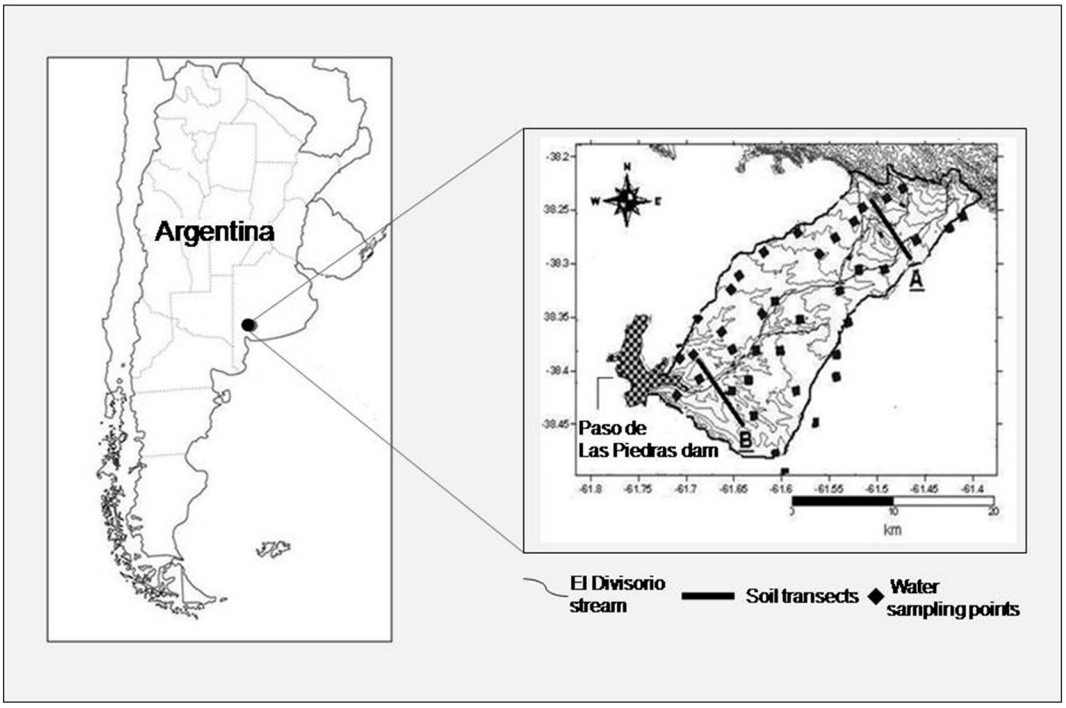

Fig. 1. Geographical situation of El Divisorio brook basin and sampling sites for soils–sediments and waters.

2006): upper basin: interfluve (S1: A–Bw–BC–2Ckm), valley slope (S2: A–AC–C1–C2–Ck) and terrace (S3: A–Bnw1–Bnw2–BCn–Cn1–2C2); middle-lower basin: interfluve (P1: A–Bt–BC–Ck–2Ckm), valley slope (P2: A–Bt–BCn–Cn–Ckn), terrace (P3: A–Bw–BCn–Cn1–Cn2) and alluvial plain (P4: A1–A2–A/Cn–Abn–ACn?–Cgn–2C). Physicochemical properties are presented in Table 2.

Geoavailability of As and other associated elements (Ba, Br, Co, Cr, Fe and Na) was analysed in disturbed samples (n: 36) collected in all the studied soil sequences. Total content for every element was determined by Instrumental Neutron Activation Analysis (INAA-Code 1D-Enhanced; detection limit 0.05 ppm, neutron flux: 7×10^{12} s^{-1}; Actlabs-Canada). Available P (P_{av}) was determined by Bray and Kurtz (1945) applying NH_4F (1 N) and HCl (0.5 N) as extractants. Iron oxides (Fe_{ox}) were determined by Mehra and Jackson (1960) applying dithionite ($Na_2S_2O_4$) as the reductant and Na citrate ($Na_3C_6H_5O_7 \cdot 2H_2O$) as a chelating agent to bind the dissolved Fe. Sodium bicarbonate ($NaHCO_3$) was used to buffer the H^+ loss during the reaction.

Parallelly, groundwaters from the phreatic aquifer were collected during the winter season to analyse their quality. Water samples with two replicates (n: 36; 500 cm^3) were taken using traditional piston pumps or windmills and also electrically-driven centrifugal pumps. Prior to transport to the laboratory, they were stored in airtight plastic bottles, labelled for identification and kept in coolers. Depth to the phreatic level was measured with a Spohr probe. Groundwater sampling points are shown in Fig. 1.

As quantification was performed with a Hydride Generator and by Inductively Coupled Plasma and Atomic Spectrometry (ICP-AES) based on the Halicz and Russell (1986). Boron and vanadium were analysed by ICP and F was determined by a specific electrode. Moreover, statistical analyses were performed. In order to identify the interrelationships between the As content in the solid phase and its presence in waters, a Principal Component Analysis was performed (PC; Infostat, Di Rienzo et al., 2013). The results are displayed in biplot graphs; however, the discussion only presents the results of those variables with a reconstruction percentage ≥ 50%.

3. Results and discussion

3.1. Soil–landscape relationships and soil macromorphology in El Divisorio basin

The multiple soil–landscape relationships identified in each section arise from the space and time variability of factors such as lithology — with superposition of aeolian and alluvial sediments — pedoclimate and relief, the latter of which controls landform stability/instability. Soil evolution is contrasting in the different sections of El Divisorio basin (Table 1). Associated with different landscape facets of the upper basin, AC or Bw horizons of S1 (interfluve), S2 (valley slope) and S3 (terrace) show lesser evolution than in P1 (interfluve), P2 (valley slope) and P3 (terrace), which have A–Bt–C morphologies in analogous landforms of the middle to lower basin. Soil parent materials are Holocene aeolian loess of medium to moderately fine textures overlying a strongly calcified 2Ckm horizon in the interfluves. In those landforms where mantle thickness reaches more than 2 m, the petrocalcic horizon was not identified within the soil sequences. Lateral continuity of loess sediments extends towards the valley terrace overlying alluvial sediments, which result in a more complex profile with a lithological discontinuity between Cn1 (silt: 353 gr kg^{-1}; sand: 429 gr kg^{-1}) and 2C2 (silt: 190 gr kg^{-1}; sand: 558 gr kg^{-1}) of S3 (Table 2). The depth of soils is moderate for S1 (<64 cm) in the interfluve zones of the upper basin, limited by the petrocalcic horizon at the base of an A–Bw–BC–2Ckm sequence. Laterally, soils respectively associated with the valley slope and with the alluvial terrace are very deep (≥2 m), with A–AC–C1–C2–Ck for S2 and A–Bnw1–Bnw2–BCn–Cn1–2C2 for S3. Melanization and biological activity promote dark colours (10YR 3/1) and the production of abundant faecal pellets in the A horizons. Pedality is moderate to strong in fine and very fine subangular blocks in the A and Bnw horizons, in the latter of which a weak clay illuviation has developed a few thin continuous clay coatings on ped surfaces. Geomorphic instability of the valley slope determines a morphogenesis–pedogenesis balance unfavourable to the latter. Thus, erosion, sediment removal and an incipient pedogenesis lead to AC

sequences having more uniform medium textures. Secondary calcification is strongly expressed through continuous cementation of the massive 2Ckm petrocalcic horizon (tosca layer, Plio–Pleistocene) of S1 and P1. The undulated topography of the 2Ckm horizon that controls soil depth denotes a relict palaeosurface inherited from more arid conditions than the present climate in the study area (González Uriarte, 1984). The tosca layer may or may not be identified in the valley slope; however, it is never present in the alluvial plain.

On the other hand, non-cemented calcite dispersed in soil mass and a strong reaction to HCl is identified in the Ck horizon of S2. In the alluvial terrace, S3 is devoid of $CaCO_3$, texture becomes finer upwards, from medium at the base to moderately fine towards the top soil. A greater wetness owing to lateral water flow stimulates a higher level of biological activity developing a moderate to strong subangular blocky structure and abundant faecal pellets in the Bnw horizon.

The sequences of the middle–lower basin have evolved into Holocene loess (P1, P2) and loess overlying moderately fine alluvial sediments (P3 and P4) (Table 1). P1 (interfluve), P2 (valley slope) and P3 (alluvial terrace) show clay illuviation and respectively include subsurface Bt and Bw horizons, the first of which has abundant continuous clay and organic matter coatings. In the alluvial plain, landscape instability and active morphogenesis caused by sedimentation processes and periodic flooding explain the lesser degree of evolution and the more complex sequence of P4, which has a buried horizon (Ab) that is a remnant of a more humid climate or the consequence of a local change of the stream base level. The A horizons have a moderately fine texture varying from silty clay loam (P1, P3) to loam (P2, P4), dark colours (10YR 3/2) and a moderate subangular blocky structure. In particular, the topsoil of P3 is a thick A horizon (44 cm) with abundant faecal pellets. Pore walls and ped surfaces of the moderately fine textured Bw horizons are coated with thick coatings composed of clay and organic matter developed by illuviation. However, the clay content increase does not satisfy the diagnostic criteria of argillic horizons. In the interfluve (P1) and in the valley slope (P2) soils have an underlying Ck formed through secondary calcification leading to $CaCO_3$ concentration in filaments, calcitic cutans, pore infillings and concretions. At the base of P1, the relict petrocalcic horizon (2Ckm, tosca layer, Plio–Pleistocene) marks the effective soil depth.

P4 is weakly developed. Nevertheless, the soil profile is much more complex than that of P1, P2 and P3. It is contaminated by aeolian deposits at the top and has gleypedofeatures (chroma ≤2); the sequence is A–A/Cn–Abn–ACn?–Cgn–2C and it is calcareous throughout due to capillary rise. Alluviation led to polygenetic evolution related to flooding, which resulted in buried horizons (Abn), lithologic discontinuities (2C)

Table 1
Soil morphology in El Divisorio basin.
Boundary: cl: clear; ab: abrupt, gr: gradual; pl: plain, un: undulated; Colour: 10 YR2/1: black; 10YR2/2: very dark brown, 10YR3/1: very dark grey, 10YR3/2: very dark greyish brown, 10YR4/1: dark grey, 10YR4/2: dark greyish brown, 10YR4/3: brown to dark brown, 10YR4/4: dark yellowish brown, 10YR5/1: grey, 10YR5/2: greyish brown, 10YR5/3: brown, 10YR6/2: light brownish grey, 10YR6/3: pale brown, Structure: bs: subangular blocky, pr: prismatic, ba: angular blocky, vf: very fine, fi: fine, m: medium, c: coarse, w: weak, mo: moderate, s: strong; Texture: L: loam, sL: silty loam, clL: clay loam, sclL: silty clay loam, SL: Sandy loam; Consistence: fri: friable, sfir: slightly firm, vfir: very firm, h: hard, vh: very hard, exh: extremely hard, Pl: plastic, ad: adhesive; Calcium carbonate: v, vestiges, vse: very slightly effervescent, se: slightly effervescent, Se: strongly effervescent; Pedofeatures: sc: scarce, f: frequent, ab: abundant, fp: faecal pellets, th: thin, cont: continuous, d:discontinuous, ccoat: clay coatings, c + om coat: clay and organic matter coatings, $CaCO_3$ features: pmy: pseudomycelium, calc: calcitans, con: concretions, inf: pore infillings.

Soil	Horizon	Depth (cm)	Boundary	Colour (moist)	Structure	Texture	Consistence	$CaCO_3$	Pedofeatures
Upper basin									
S1 — Interfluve	A	0–30	cl, pl	10YR3/2	bs, vf,mo, fi, m–w	sL	fri to h	se	ab, fp
	Bw	30–50	cl, pl	10YR4/3	bs, f–vf, s	L	h	vse	sc, th,d, ccoat
	BC	50–64	ab, un	10YR4/4	bs, m, mo	L	vfir	vse	–
	2Ckm	64+	Petrocalcic horizon						
S2 — Valley slope	A	0–20	cl, pl	10YR3/1	bs, vf–m, mo	L–clL	fri	v	f, fp
	AC	20–55	cl–gr, pl	10YR3/2	bs, c–m, mo–w	clL	sfir	v	f, fp
	C1	55–110	cl, pl	10YR4/3	bs, fi–m, w	clL	fir	v	–
	C2	110–142	cl, pl	10YR4/3	bs, fi, w	clL	fir	v	–
	Ck	142–200		10YR4/3	bs, fi, w		fir	Se	–
S3 — Terrace	A	0–38	cl–gr, pl	10YR3/1	bs, vf, mo	sclL	h	v	ab, fp
	Bnw1	38–82	cl–gr, pl	10YR4/1	bs, c, s	sL	h	v	sc, fp
	Bnw2	82–143	cl–gr, pl	10YR4/2	bs, m, mo–s	sL	h	v	sc, fp
	BCn	143–170	cl–gr, pl	10YR4/3	bs, vf, w–mo	L	fri	v	
	Cn1			10YR4/3		cL		v	
	2C2			10YR4/3				v	
Middle–lower basin									
P1 — Interfluve	A	0–18	cl, pl	10YR3/2	bs, fi–vf, mo	cL	fri	–	ab, fp
	Bt	18–73	cl, pl	10YR3/1	pr, fi–m, s	c	vh	–	ab, cont, c + om coat.
	BC	73–88	ab, pl	10YR4/3	bs,fi–vf, s	cL	vh	–	sc, ccoat
	Ck	88–108	ab, un	10YR5/3	bs,fi–vf, s		vh	Sef	pmi, calc, nod, con of $CaCO_3$
	2Ckm?	108+	Petrocalcic horizon?						
P2 — Valley slope	A	0–23	cl, pl	10YR3/2	bs, f–vf, mo	L	vh	–	ab, fp
	Bt	23–40	cl, un	10YR4/2	bs,m–c, mo	L	vh	–	ab, c + om coat
	BCn	40–54	cl, un	10YR4/2	bs, fi–vf, mo	L	vh	–	s, ccoat
	Cn	54–73	ab, un	10YR4/3	bs, m, w	L	vh	–	
	Ckn	73–112+		10YR6/2	bs, m–c, mo	SL–sL	vh	Sef	ab, pmy, calc, con, inf of $CaCO_3$
P3 — Terrace	A1	0–12	cl, pl	10YR2/1	bs, vf, mo	scL–sL	h	–	ab, fp
	A2	12–44	cl, pl	10YR2/1	bs, m–fi, mo	sL	h	–	ab, fp
	Bw	44–76	cl, pl	10YR5/2	bs, m–fi;s–mo	sL	h	–	s, c + om coat
	BCn	76–117	cl–gr, pl	10YR5/2	ba, m, mo	sL	fir	–	s, ccoat
	Cn1	117–200	gr, pl	10YR6/2		L		v	
	Cn2	200+		10YR6/3				v	
P4 — Flood plain	A	0–18	cl, pl	10YR5/2	bs, vf, mo	sL	h	v	ab fp
	A/Cn	18–51	cl, pl	10YR5/2	bs, vf–c, mo	scL	fir	v	
	Abn	51–81	gr, pl	10YR2/2	bs, fi–m, w–mo	scL	fir	sef	ab fp
	ACn?	81–111	gr, pl	10YR5/2		scL	Pl, ad	sef	
	Cgn	111–181		10YR5/2		sL	Pl, ad	Sef	
	2C	181+	Very fine gravel layer						

interspersed in the soil sequence and an underlying layer of fine gravel at a depth of 180 cm. The soil moisture regime is udic/aquic and gleying pedofeatures appear in the subsoil (Cg).

S3, P2, P3 and P4 are non-saline sodic soils developed in landforms shaped by fluviatile dynamics where alluviation and gleying caused different degrees of sodicity. Their chemistry is characterized by high pHs and elevated levels of exchangeable sodium percentage (ESP) that particularly affect soils of the valley slope, the terrace and the flood plain of the middle–lower basin, where soils are moderate to strongly sodic mainly in depth (Table 2).

3.2. Soil classification (Soil Survey Staff, 2014)

In the stable interfluve of the upper basin, although the moisture regime is udic, S1 is slightly calcareous throughout since leaching was insufficient to deplete $CaCO_3$ from the profile. S1 is a Petrocalcic Calciudoll fine-loamy, mixed, thermic. It has a mollic epipedon (0–30 cm) followed by a Bw cambic horizon (30–50 cm) and a 2Ckm petrocalcic horizon (64+ cm) as subsurface diagnostic horizons. S2 is classified as a Typic Calciudoll coarse loamy, mixed, thermic. The surface horizon is a mollic epipedon (0–20 cm) and the Ck horizon is calcareous, non-calcic. The landscape position is unfavourable to pedogenesis and subsurface diagnostic horizons are not identified. S3 is located in the terrace, where sodicity is a common limitation (ESP: 19.8–21.9%), and is classified as Typic Hapludoll clayey, mixed, thermic with a sodic to strongly sodic subsoil phase. The diagnostic horizons are a mollic epipedon (0–38 cm) and a cambic horizon (38–143 cm) with a moderate to strong subangular blocky structure.

P1 is a Calcic Argiudoll fine-clayey, mixed, thermic. It has a mollic epipedon overlying a 55-cm thick argillic Bt; clay coatings are frequent and clay content satisfies the argillic diagnostic criteria. It is followed by a calcic horizon with frequent secondary calcite pedofeatures superposed to a 2Ckm?, which has a high $CaCO_3$ content and is partially cemented. Associated with the valley slope of the middle–lower basin, P2 is a Calcic Argiudoll fine-loamy, mixed, thermic sodic to strongly sodic subsoil phase. The A horizon qualifies as a mollic epipedon and the subsurface diagnostic horizons are an argillic Bt horizon and a calcic Ckn horizon with elevated Na^+. Sodicity ranges from 40 cm up to 112 cm in depth.

P3, located in the valley terrace, is classified as a Typic Hapludoll fine clayey, mixed, thermic, strongly sodic subsoil phase. At the top it has a mollic epipedon; clay coatings are identified in the Bw horizon but clay content is not enough to qualify as an argillic horizon. From a depth of 76 cm, ESP ranges from 66.4% in BCn up to 40.1% in the Cn2 and the soil is non-saline and strongly sodic.

The morphology and genesis of P4 harmonize with its landscape position and with alluvial sedimentation that result in lithologic discontinuities and a buried soil. The moisture regime is aquic; on the surface it has an ochric epipedon and no subsurface diagnostic horizons are identified. P4 is classified as Aquic Udifluvent fine loamy, mixed, thermic. Risk of flooding, poor to very poor drainage and a high Na concentration are its main limitations for agricultural production.

Table 2
Soil physicochemical properties (upper basin and middle–lower basin).

	Horizon	Depth (cm)	Texture (gr kg^{-1})			CEC ($cmol_c$ kg^{-1})	Exchangeable complex ($cmol_c$ kg^{-1})				pH 1:2.5		ESP (%)	P_{av} (mg g^{-1})
			clay	silt	sand		Ca^{2+}	Mg^{2+}	Na^+	K^+	H_2O	KCl		
Upper basin														
S1 — Interfluve	A	0–30	266	376	358	17.8	—	—	0.5	2.1	8.1	5.1	2.8	4
	Bw	30–50	486	190	324	18.8	—	—	0.5	1.8	7.2	5.3	2.7	1
	BC	50–64	265	451	284	18.6	10.3	4.4	0.5	1.4	7.5	6.3	2.7	2
	2Ckm	64+	81	203	716	10.8	10.5	4.8	0.8	1	8.8	7	7.4	1
S2 — Valley slope	A	0–20	153	259	588	12.2	4.9	2.5	0.4	2.4	6.5	5.6	3.3	9
	AC	20–55	169	238	593	12.6	5.3	3.9	0.4	1.4	6.4	5.5	3.2	5
	C1	55–110	195	221	584	12.8	4.8	6.2	0.5	1.2	7	5.7	3.9	7
	C2	110–142	169	260	571	11.6	4.7	5	0.5	1.3	7.3	5.8	4.3	4
	Ck	142–200	201	244	555	1.8	—	—	0.5	1.3	8.5	7.1	4.2	3
S3 — Terrace	A	0–38	466	387	147	22.7	—	—	1.9	1	7.7	6.2	8.4	12
	Bnw1	38–82	404	481	115	21.7	—	—	4.3	1.3	8.2	6.4	19.8	23
	Bnw2	82–143	314	483	203	17.7	—	—	7.1	1.5	8.6	6.5	40.2	13
	BCn	143–170	315	417	268	17.5	—	—	6.8	1.5	8.2	6.6	38.8	14
	Cn1		218	353	429	15.9	—	—	3.5	1.3	7.8	6.3	21.9	11
	2C2		252	190	558	8.9	—	—	0.8	0.5	8.3	7.1	9.3	7
Middle–lower basin														
P1 — Interfluve	A	0–18	358	504	138	17.4	6.2	4.7	0.5	2.3	6	5.1	2.9	39
	Bt	18–73	486	450	64	24.2	9.2	10.3	0.8	2.8	6.8	5.3	3.3	11
	BC	73–88	257	666	77	29.8	—	—	1.2	4.7	7.5	6.3	4	27
	Ck	88–108	430	482	88	26.7	—	—	1.3	4.6	8.3	7	4.9	15
	2Ckm?													
P2 — Valley slope	A	0–23	142	338	520	11.4	4.3	3.3	0.6	2	6.3	5.3	5.3	6
	Bt	23–40	307	304	389	15.7	5.2	6.3	0.9	2.5	6.8	5.3	5.7	9
	BCn	40–54	272	627	101	14.8	4.5	5.9	2.2	1.8	7.2	5.4	14.9	3
	Cn	54–73	309	300	391	15.6	—	—	5.8	1.7	7.9	6	37.1	3
	Ckn	73–112	345	320	335	17	—	—	11.9	1.9	9.9	7.9	70.1	1
P3 — Terrace	A1	0–12	387	464	149	20.2	6.9	6.2	0.7	3.4	6.5	5.6	3.5	29
	A2	12–44	284	643	73	22.3	7.5	9.3	0.9	3	8	5.8	4	9
	Bw	44–76	289	630	81	21.9	—	—	2.6	1.9	7.9	6.3	11.9	18
	BCn	76–117	271	627	102	22.9	—	—	14.9	2.2	9.4	7.3	66.4	16
	Cn1	117–120	274	521	205	18.4	—	—	12.5	1.8	9.2	6.9	67.8	19
	Cn2	120–187	193	409	398	14.2	—	—	5.7	1.4	8.7	6.5	40.1	24
P4 — Flood plain	A	0–18	221	293	486	14.1	—	—	1.2	2.2	7.9	6.9	8.5	39
	A/Cn	18–51	176	482	341	19.5	—	—	3.9	1.7	8.1	7	19.9	32
	Abn	51–80	261	415	324	17.6	—	—	9.1	1.3	9.2	7.5	51.6	12
	ACn?	80–110	190	519	291	17.3	—	—	4.3	1	8.3	6.7	24.9	9
	Cgn	110–180	122	570	308	17.4	—	—	4	1.5	8.2	6.7	22.9	11

3.3. Soil mineralogy and provenance sources

The total sand fraction comprises 95% of light and 4–5% of heavy minerals. The most frequent light constituents are usually fresh or slightly weathered quartz, orthoclase, plagioclase, acid volcanic glass, biotite and muscovite, phytolites and lithic fragments. All the soils have comparable amounts of volcanic glass ranging from 1 to 20%.

The volcanic glass separated from the loess and loess-derived soils shows a typical rhyolite composition. Opaques, epidote, augite, hypersthene, lithic fragments, green hornblende and scarce brown hornblende constitute the heavy subfraction.

Although the mineral suite does not reflect lithological discontinuity (Blanco et al., 1997), proving similarity of parent materials, variability in the rhythm of transport and sedimentation that influenced the sorting processes introduces quantitative differences in some constituents. Clay and silt minerals show similarity too. Illite (1.0 nm) is dominant together with irregular mixed layers of illite–smectite (2.4 nm) and/or chlorite–smectite (2.75 nm). Variable amounts of low-crystallinity minerals such as iron oxides and very fine volcanic glass are identified in the fine fraction (<2 μm). Neoformed kaolinite is low despite the udic moisture regime.

Aeolian dynamics carried particles by saltation and suspension and deposited different amounts of sediments of variable granulometry over several aeolian pulses during the Holocene (Amiotti et al., 2001; Blanco and Sánchez, 1994). Due to a similar provenance of the loess sediments, the intra- and interpedon mineral association of the sand fraction shows qualitative homogeneity. The mineral constituents are of primary aeolian origin sourced from near areas located in the distal alluvial plain of the Colorado river and remote zones situated in the southern Andes range and Extra-Andean Patagonia, transported by W-SW winds towards the depositional areas in the southern Pampean region (Zárate, 2003; Zárate and Tripaldi, 2012). The present-day aeolian dust collected in the study area confirms exportation from close and remote sources (Gaiero et al., 2004).

Loess deposits, landform configuration and the chronological factor depending on the residence time of water in every main landform and microlandform play a role in the geographical distribution of As concentrations in surface and groundwaters (Blanco et al., 2012). The interaction of the phreatic aquifer with loess sediments and loess-derived soils containing from 5.10 to 20.70 mg kg^{-1} of As in the sand fraction is conducive to As release from the solid to the aqueous phase (Table 3). No discrete As minerals were identified petrographically in any of the studied fractions, from which it may be surmised that As is hosted in the crystalline structure of some primary minerals by isomorphic substitution.

3.4. Arsenic and associated elements in the soil–sediment matrix

The total contents of As, Ba, Cr, Co, Fe, Na and Fe_{ox} obtained for the solid phase in the studied soils and sediments of the El Divisorio brook are presented in Table 3 and their mean contents for the upper and middle–lower sections of the basin are shown in Table 4. Total As contents range from 5.80 to 12.20 mg kg^{-1} for the upper basin areas. In general terms, S2 in the valley slope presented the lowest amounts of As in accord with a morphogenesis-pedogenesis balance favourable to the former, which yielded a lower frequency of As-bearing minerals than that of other soils in the same section.

Table 3
Total contents of As, Ba, Br, Co, Cr, Fe and Na in soils—sediments of El Divisorio Basin (Buenos Aires province, Argentina).

	Horizon	As mg kg^{-1}	Ba mg kg^{-1}	Br mg kg^{-1}	Co mg kg^{-1}	Cr mg kg^{-1}	Fe %	Na %	Fe_{ox} ppm
Upper basin									
S1	A	9.20	530	16.40	13	38	3.05	1.56	152.25
	Bw	8.20	490	29.50	14	38	3.85	1.70	243.25
	BC	9.10	430	18.50	14	49	3.78	1.77	182.35
	2Ckm	9.90	310	17.90	7	35	2.07	1.02	36.75
S2	A	6.20	530	8.50	11	44	3.04	2.24	180.25
	AC	5.80	460	12.90	10	40	3.3	2.19	259.00
	C1	5.80	590	9.60	11	43	3.99	2.24	127.75
	C2	8.20	480	6.60	12	42	3.91	2.28	141.75
	Ck	9.00	390	4.30	11	39	3.54	2.25	82.25
S3	A	10.30	480	34.40	14	36	3.71	1.42	414.75
	Bnw1	9.60	480	24.80	14	36	3.67	1.42	400.75
	Bnw2	7.30	460	15.30	16	35	3.64	1.75	309.75
	BCn	7.30	460	9.90	13	38	3.49	1.95	264.77
	Cn1	11.20	410	3.60	13	39	3.64	1.95	227.50
	2Cn2	12.20	450	2.30	10	35	3.24	1.58	194.25
Middle–lower basin									
P1	A	6.50	200	15.30	18	34	3.85	1.46	420.00
	Bt	9.30	390	33.00	18	39	4.56	1.10	278.25
	BC	8.90	410	10.30	16	41	4.99	0.91	180.25
	Ck	9.00	490	5.90	16	45	4.75	1.06	145.25
P2	A	6.10	480	8.30	11	38	3.55	2.04	182.00
	Bt	7.00	460	17.30	13	36	4.13	1.81	183.75
	BCn	6.80	450	10.40	13	38	3.91	1.88	133.00
	Cn	5.10	290	6.60	13	50	3.99	2.06	113.75
	Ckn	7.80	450	6.40	14	35	3.67	1.76	63.00
P3	A1	8.90	180	14.10	15	36	3.17	1.41	351.75
	A2	10.10	460	39.50	19	31	3.68	1.16	351.80
	Bw	9.00	310	22.10	18	33	4.18	1.26	400.75
	BCn	12.70	530	8.40	16	29	4.21	1.63	304.50
	Cn1	12.40	480	5.80	14	40	3.88	1.75	208.25
	Cn2	10.40	450	2.10	14	35	4.04	2.13	120.75
P4	A	9.30	430	9.30	14	39	3.47	1.95	1053.50
	A/Cn	11.20	410	21.30	14	43	3.33	1.81	652.75
	Abn	12.00	340	15.50	14	34	3.51	1.92	509.25
	ACn?	20.70	300	7.90	15	70	3.52	1.70	381.50
	Cgn	18.40	490	5.30	14	46	3.68	1.69	182.00
	2C	13.20	350	4.10	11	30	2.82	1.40	327.25

Table 4
Mean contents of As, Ba, Br, Co, Cr, Fe and Na in soils—sediments of the studied basin.

Element	As mg kg^{-1}	Ba mg kg^{-1}	Br mg kg^{-1}	Co mg kg^{-1}	Cr mg kg^{-1}	Fe %	Na %
Upper basin	8.62	463.33	14.30	12.20	39.13	3.46	1.82
Lower basin	10.23	397.72	12.80	14.76	39.14	3.85	1.61
General average	9.55	425.00	13.42	13.70	39.14	3.69	1.70

Intraprofile variability of As levels is low for S1, as evidenced by the slight decrease in the Bw horizon (A: 9.20 mg kg^{-1}; Bwn: 8.20 mg kg^{-1}) owing to low weathering, minor lixiviation and moderate pedogenesis. S3 associated with the alluvial terrace shows a similar trend (A: 10.30 mg kg^{-1}, Bw: mean 8.40 mg kg^{-1}, C: 11.20 mg kg^{-1}, 2C2: 12.20 mg kg^{-1}). Fixation of As through a mechanism analogous to phosphate adsorption into calcite (Alexandratos et al., 2007) may occur in the relict 2Ckm petrocalcic horizon of S1, which has an As content (9.90 mg kg^{-1}) comparable with that of the Ck horizons of S2 (valley slope, upper basin, As: 9 mg kg^{-1}) and of P1 (interfluve, middle–lower basin, As: 9 mg kg^{-1}). Previous studies have informed of a lower As amount in the solid phase of the petrocalcic horizon (Plio–Pleistocene) (Blanco et al., 2006, 2011). In spite of the fact that the As contents in the studied area do not reflect the marked chronological discontinuity existing at the depth of the 2Ckm petrocalcic horizon, the Ba, Co, Cr and Fe contents show a sensitive decrease here (Table 3). 2Ckm and Ck horizons show higher As contents in the correspondent profile; nevertheless, they exhibit lower amounts compared with the other younger C horizons in soils associated with either the unstable flood plain or the terrace. This variability could be attributed to differences in the surface age and in the residence time of water. In more stable landforms, an older surface age and a longer period of time subject to the weathering process led to lower As contents in the calcareous horizons. The most elevated As contents were detected in the other C horizons associated with unstable landforms such as the flood plain or the terrace. In the terrace, stable at present although unstable in the past, the aqueous phase is in contact with younger sediments, the water residence time is shorter and, consequently, weathering is less expressed. Hence, As contents in the solid phase are controlled too by the chronological factor. In addition, differences in the surface age and in the residence time of water lead to variability of As contents conducted by the morphogenesis–pedogenesis balance in every landform or microlandform depending on their stability.

Comparatively speaking, As contents slightly augment from soils of the recharge areas in the upper basin (range: 5.80–12.20 mg kg^{-1}) towards those of the discharge in the middle–lower basin (range: 5.10–20.70 mg kg^{-1}). This spatial variability is attributed to the intrabasin pattern that sediment pulse dynamics imprints to aeolian loess distribution through the interfluve plain and the valley slopes and to the dynamics of the loess-derived alluvial sediments along the landforms within the valley. Mineral sorting during transport leads to differences in the frequency of occurrence of As-bearing constituents, which is reflected in the geographic variability of total As contents (Blanco et al., 2006).

Nonetheless, in some soils with differentiated profiles, As levels are conditioned by pedogenetic processes and derived soil properties such as clay translocation and the amount of illuvial clay and/or leaching concentration of $CaCO_3$ (Roca et al., 2012). The Bt horizon of P1 concentrates 9.30 mg kg^{-1}, exceeding the As content in the A, BC, and Ck horizons. The vertical clay translocation and its accumulation through illuviation in the Bt horizon increases the geoavailable As both hosted in the primary sand particles and particularly associated with illuviated clay. The Bw horizon of P3 presents a similar As content. P2 morphology is similar to P1; however, since it has a lower clay amount, Bt showed a decreasing As content of about 25% (As: 7 mg kg^{-1}). The C horizons, comparable to sediments of provision sources, normal As contents were found and never have an excessive As geoavailability. The alluvial dynamics is reflected in a more irregular vertical distribution of As, which in P4 oscillates between 9.30 and 20.70 mg kg^{-1}. In this profile, a lower content of As was determined in the solid phase of the A horizon (As: 9.30 mg kg^{-1}). The aquic soil moisture regime caused by flooding and capillarity promotes mineral dissolution in the Cg horizon contributing to the removal of As from bearing minerals in the solid phase and to its incorporation via leaching into the soluble phase of the phreatic aquifer (Table 3).

In addition, the soils situated on the valley slopes have similar mean contents of geoavailable As (S2: 7 mg kg^{-1}, P2: 7.80 mg kg^{-1}), which are the lowest mean value within the studied basin. The instability associated with landform fosters erosion and the removal of As-bearing minerals, which are reflected in decreasing As amounts when compared with more stable landscape positions.

In all cases, As contents were considered background levels. Nevertheless, total geoavailable As is not an effective indicator of its bioavailability (Xie and Naidu, 2006). The origin and the spatial distribution of geoavailable As and the mobility of bioavailable As towards the shallow aquifer are mainly controlled by lithology, hydrochemistry and geochemistry of soils and sediments on a local scale (Blanco et al., 2006). Scavenge of As from the As-bearers and its release from the mineral structure brings about bioavailable As, which is further incorporated into the aqueous phase. Here, the main influential variables affecting As bioavailability are the As content, the amount and type of clay, the soil reaction, the adsorption–desorption processes and competition with other ions in every landform, all of them controlling the entry of released As into the aquifer as well as its mobility, intrabasin spatial variability and transference to crops and human food (Fitz and Wentzel, 2006; Garnier et al., 2010).

The vertical and lateral spatial variability of mean As contents and other associated elements in the solid phase appears to be essentially governed by geopedogenetic complexity owing to aeolian and fluviatile processes that impose mobilization, sorting and deposition of minerals, causing a major concentration of As-bearers in the lower basin. However, postsedimentary pedogenesis and soil evolution had an effect on the intraprofile distribution of As, particularly in the most developed soils differentiated by clay illuviation and leaching and by secondary accumulation of $CaCO_3$ at the bottom of the sequences. A less aggressive hydrochemical environment in the upper basin than in the middle–lower one promotes in the former greater mineral stability and moderate silicate hydrolysis. Consequently, in the recharge areas, the solid phase retains As and Na in the crystal structure of the mineral components of the coarse fraction whilst lower amounts of As are released into the soluble phase. Sodium is a common element that is part of the crystalline structure of the calcosodic plagioclases, which are found in a higher proportion in the upper basin.

On the other hand, Na and/or CO_3 concentrations in water control pH together with the transference of As to hydric resources, thus increasing its concentration along the water flow. A progressively more alkaline hydrochemistry and a more aggressive weathering environment along the flow contribute to the removal of As and other elements from the crystalline phase, which increase their concentration as soluble components longitudinally from the recharge area of the aquifer to its discharge in the middle–lower basin, reaching levels above the guide value (10 μg L^{-1}) in this landscape segment.

Fe_{total} and Fe_{ox} were found in higher contents towards the lower basin owing to sedimentation (Fe_{total}) and weathering and subsequent oxidation (Fe_{ox}). Oxidation contributes to the segregation of Fe_{ox} that mainly integrates the fine fraction of the soils; oxidizing Fe species

also control the levels of As transferred to waters. After release from the crystal structure, at elevated pHs as those found in the middle–lower basin, entry of As into the aqueous phase and its concentration is enhanced by desorption from Fe_{ox}, which is also controlled by CO_3–HCO_3 chemistry.

Climate is another important factor regulating the levels of As and other associated elements in waters of the semiarid–subhumid transition. In the shallow aquifers, As levels increase in the summer season due to evaporation associated with water deficit, the occurrence of intense and prolonged dry phases, erratic rainfall and a greater probability of high winds with a higher evaporative power. Also, during winter, the lower contribution of precipitation limits the dilution effect, thereby leading to elevated concentrations of As in the aqueous phase.

3.5. Hydrochemical characteristics of the phreatic aquifer

The phreatic aquifer is multilayered. Surface and ground waters are sodium-bicarbonated and their quality decreases along the flow from C_3S_2 (high salinity and low to medium sodium hazard) in the recharge area (upper basin) to C_3S_3 (high salinity and medium to high sodium hazard) in the discharge area (middle–lower basin) in accord with higher levels of Na^+ (upper basin: 13.220 μg L^{-1}; lower basin: 18.770 μg L^{-1}) and salinity (upper basin: 1.04 dS m^{-1}; lower basin: 1.54 dS m^{-1}). Electrical conductivity varied from 1.04 dS m^{-1} to 1.54 dS m^{-1} in the same direction, being higher during the spring–summer period due to evaporative processes (Espósito et al., 2011). The mean residual sodium carbonate (RSC) was >2.5 mmol L^{-1} and showed spatial and time variability presenting highly significant differences ($p < 0.01$) within the basin, with increments during the summer in view of lower precipitation and reduced recharge. Hardness varied from 69.28 ppm to 66.90 ppm. More than 90% of phreatic waters have As exceeding the guide value (Tables 5 and 6) in the range of 10 to 114 μg L^{-1} (mean: 56 μg L^{-1}) coexisting with other trace elements such as B ranging from 120 to 1420 μg L^{-1}(mean: 797 μg L^{-1}), F in the range of 200 to 6600 μg L^{-1} (mean: 2610 μg L^{-1}) and V from 40 to 800 μg L^{-1} (mean: 392 μg L^{-1}). Although high concentrations were determined in the whole basin, the highest levels indicative of the worsening of water quality were detected particularly in areas of the middle–lower basin (Table 6). Spatial and time variability of As concentrations and the associated groundwater toxicity could be attributed to a longer residence time of water in contact with the aquifer lithology in the lower basin. Hence, silicate hydrolysis, oxido-reduction that releases As from the solids and/or adsorption–desorption and formation of complex ions in the fine fraction (<2 μm) lead to unacceptable levels in certain landscape positions conducive to a heterogeneous and patchy spatial pattern. Once As ions have been released from the mineral phase into groundwaters, several factors such as landform configuration, climate and pedoclimate, the residence time of water in every landform, the local hydrogeochemical variables (pH, Eh, DO, EC, competition with other ions, adsorption–desorption) control As mobility and its concentration in a dynamic equilibrium with the local chemistry in every landscape position (Blanco et al., 2006).

3.6. Evaluation of As behaviour in the solid and aqueous phases

The highest mean As values were obtained for the solid phase of the soils in the middle–lower positions with respect to the upper section (Table 4; As, upper section: 8.62 mg kg^{-1}; middle–lower section: 10.23 mg kg^{-1}). An analogous behaviour was measured in the aqueous phase; however, differences were not statistically significant. The analysis of the groundwater samples collected in the upper section and in the middle–lower basin respectively gave 20 μg L^{-1} and 52 μg L^{-1} mean As concentrations (Table 5).

Table 5
Mean As, V, B and F concentrations (μg L^{-1}) in groundwaters in the studied basin.

	As μg L^{-1}	V μg L^{-1}	B μg L^{-1}	F μg L^{-1}
Upper basin	20	446	880	2761
Middle–lower	52	591	785	3000
General average	56	392	797	2610

Table 6
Concentrations of As, B, F and V in groundwaters of El Divisorio Basin (samples: upper basin, n: 12; middle–lower basin: n: 24).

Element	As	V	B	F
Basin	μg L^{-1}	μg L^{-1}	μg L^{-1}	μg L^{-1}
Upper	30	190	607	1320
	19	140	880	900
	10	400	120	200
	26	400	220	400
	13	400	290	660
	43	150	510	690
	71	150	310	590
	21	130	600	980
	26	220	660	1240
	29	230	640	1570
	24	150	660	1280
	0	40	600	1000
	60	500	820	4280
	60	510	820	4860
	50	460	630	2350
	60	510	1000	6600
	49	540	1420	4630
	72	150	830	3160
	55	300	610	2500
	83	740	690	3240
	56	240	840	3210
	88	800	740	3000
	55	310	550	1510
	76	660	970	2360
Middle–lower	99	320	1100	4400
	53	490	910	2560
	85	650	850	3090
	56	540	890	2000
	69	590	810	2750
	36	290	1180	2040
	54	580	990	4880
	54	450	950	1730
	32	140	760	2280
	68	550	1010	3930
	114	740	720	3230
	27	270	930	670

3.6.1. Principal Component Analysis applied to the solid phase (soils–sediments)

The correlation analysis between the studied variables (As, Ba, Br, Co, Cr, Fe and Na) and the first three principal components (PC) permitted to identify quantitative differences in the chemical composition of the solid phase for the different landscape positions within the basin. Eigenvalues were: 1 (0.31), 2 (0.21) and 3 (0.19). The two first principal components (PC1 and PC2) aiding the graphical representation of elements determined for every horizon on same plane, explain 52% of the total variability. The variables with the highest contribution to PC1 were Br (0.673), Co (0.868) and Na (−0.769). The variables As (0.814) and Cr (0.686) were the most important for PC2, while Ba (0.504) and Fe (0.783) were the most important for PC3 (Table 7).

Table 7
Correlation between the analysed variables and the first three Principal Components (PC) in soils–sediments.

	As	Ba	Br	Co	Cr	Fe	Na
PC1	0.07	−0.26	**0.67**	**0.87**	0.22	0.52	**−0.77**
PC2	**0.81**	−0.45	−0.28	0.09	**0.69**	−0.09	−0.16
PC3	−0.04	**0.50**	−0.26	0.30	0.43	**0.78**	0.35

Bold data are variables having a higher contribution to formation of each PC.

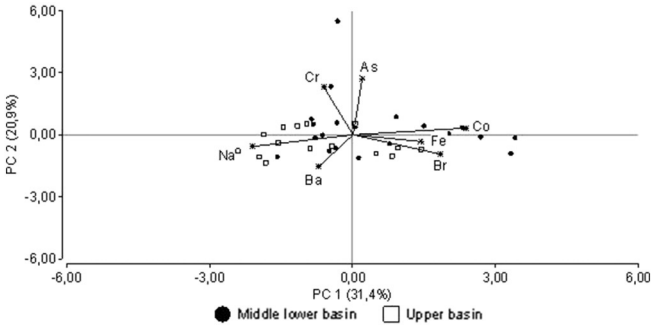

Fig. 2. Biplot PC1–PC2 in soils–sediments.

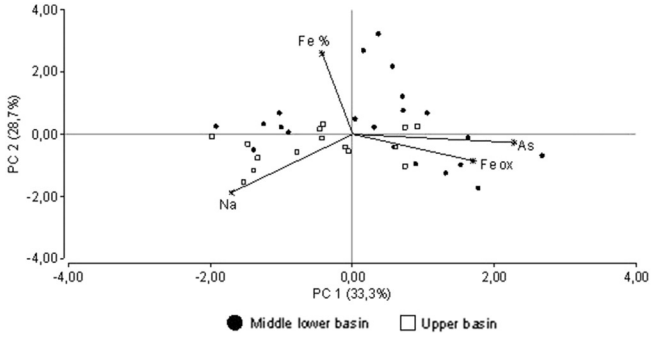

Fig. 4. Biplot PC1 and PC2 for As, total iron (Fe tot), iron oxides (Fe ox) and Na in soils–sediments.

Fig. 2 is a biplot PC1–PC2, which shows, in general terms, the contents of Br and Co higher than the mean values (Br: 13.42 mg kg^{-1}; Co: 13.70 mg kg^{-1}, Table 4) found for soils of the lower basin toposequence and, particularly, detected for the A2 horizon (12–44 cm) of P3 (Br: 39.50 mg kg^{-1}, Co: 19 mg kg^{-1}) in the alluvial terrace and for the Bt horizon (18–73 cm) of P1 (Br: 33 mg kg^{-1}, Co: 18 mg kg^{-1}) in the interfluvial plains (Table 3). The AC horizon of P4 in the alluvial terrace has As and Cr exceeding the mean value (As: 9.55 mg kg^{-1}, Cr: 39.14 mg kg^{-1}). When contrasting the intrabasin spatial distribution of As, Fe, Co, Br, Cr, Na and Ba, PC1 and PC2 showed that the solid phase in the upper basin had higher contents of Na and Ba, which were also more elevated than the total amounts in the lower section of El Divisorio stream. The remaining elements (As, Fe, Co, Br and Cr) yielded larger amounts in the soils associated with the different landforms of this section as a consequence of particle selection by size and density conducive to a greater concentration of As-bearing minerals.

The second biplot (PC1 and PC3, Fig. 3) shows that the variables with a percentage of reconstruction higher than 50% are, as in the previous case, Br and Co, to which Fe and Na are now added. The contents of Na and Br in the solid phase of the soils belonging to the middle–lower basin are lower (Na: 1.61%, Br: 12.80 mg kg^{-1}) than the intrabasin average ones (Na: 1.70%; Br: 13.42 mg kg^{-1}) (Table 4).

3.6.2. Geoavailability of As, Fe_{total}, Fe_{ox} and Na in the solid phase of soils: Principal Component Analysis

In each basin segment, quantitative differences in the chemical composition of the solid phase were demonstrated by the correlation analysis between As, Fe_{total}, Fe_{ox}, Na and the three first PC. PC1 and PC2 explain 60% of the total variability (Fig. 4). The cophenetic correlation coefficient was 0.96, being a dimension of the quality of the reduction achieved by calculating the correlation between the Euclidean distances and the reduced space and these distances in the original space of a dimension given by the original variables (Di Rienzo et al., 2013). Eigenvalues were: 1 (0.33), 2 (0.29) and 3 (0.22). The variables that contributed most to PC1 were As (0.79) and Na (−0.60); Fe_{total} (0.80) and Na (−0.60) were relevant to PC2, whilst PC3 was mostly contributed by Fe_{ox} (0.75) (Table 8). Fe_{total} and Fe_{ox} geoavailability is provided by different hosting subfractions of the solid phase. Fe_{total} is related to primary constituents mainly of the sand fraction represented by heavy minerals, including ilmenite and magnetite among the opaque minerals, together with transparent such as augite, green hornblende, hypersthene, epidote and scarce tourmaline. The Fe_{ox} constituents are also hosted in the fine fraction (Blanco and Sánchez, 1994).

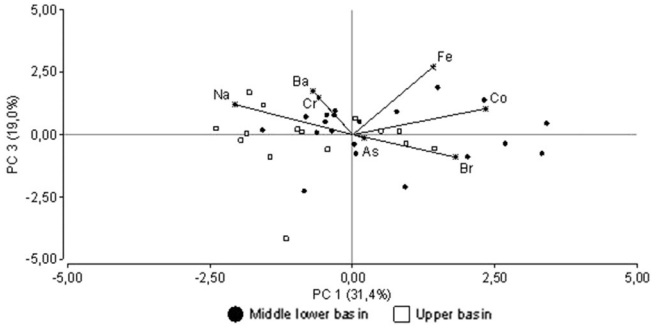

Fig. 3. Biplot PC1–PC3 in soils–sediments.

According to the PC1–PC2 biplot (Fig. 4), PC1 is explained mainly by As. Fe_{total} and As yielded more elevated contents in the middle–lower toposequence, being higher than their respective intrabasin average values, particularly in the AC horizon (As: 20.7 mg kg^{-1}) of the alluvial plain soil sequence and in the BC horizon (Fe_{total}: 4.99%) and Ck horizon (Fe_{total}: 4.75%) of the interfluves (Table 3).

Regardless of the excessive As concentrations in groundwaters, intrabasin geoavailable As was normal (range: 5.10–20.7 mg kg^{-1}). In the lower basin, the minimum values correspond to the C horizon of the sequence associated with the valley slope and the maximum ones were for the AC horizon of the alluvial plain. In this area, the maximum contents of As found in the solid phase of soils of the lower basin correlate to excessive As levels (>10 μg L^{-1}) in the phreatic aquifer (Espósito et al., 2010).

Volcanic glass is considered the main source of As supply to phreatic groundwaters (Nicolli et al., 2012). However, it may not be the only constituent that provides this natural contaminant to water resources of the southwestern Pampa. The primary source of As supply to water are the minerals of the loess sand fraction, which also include volcanic glass, being the mineral association of the clay fraction a source of an important additional As input to groundwater (Blanco et al., 2011). On the other hand, the average geoavailable Na (1.82%) in the soils of the upper basin landforms slightly exceeds that of the lower basin (1.61%). In the former, the valley slope soil renders an average 2.24% derived from a greater contribution of calcosodic plagioclase (albite, andesine) hosting Na in the coarse mineral constituents for the upper basin segments. Iron in the form of oxidizing components controls As levels transferred to waters, whilst Na, in addition to carbonates, determines the pH, being another control factor of As availability and transfer to groundwaters in every basin segment. The multiple soil–landscape relationships are ascribable to the chrono-spatial variability of lithology with juxtaposed aeolian and alluvial sediments, soil climate and relief, the latter of which controls the morphogenesis–pedogenesis balance according to landform stability–instability and the intrabasin

Table 8
Correlation between Fe_{ox}, Fe_{tot}, Na, As and the first three Principal Components (PC).

	Fe_{ox}	Na	As	Fe_{total}
PC1	0.59	**−0.59**	**0.79**	−0.15
PC2	−0.20	−0.60	−0.09	**0.80**
PC3	**0.75**	0.22	−0.33	0.37

Bold data are variables having a higher contribution to formation of each PC.

Table 9
Correlation between the studied variables and the first three Principal Components (PC) in waters.

	As	B	F	V
PC1	**0.82**	**0.75**	**0.87**	**0.89**
PC2	−0.49	0.60	0.21	−0.25
PC3	0.02	−0.25	0.44	−0.20

Bold data are variables having a higher contribution to formation of each PC.

distribution of As-bearing minerals. A larger amount of Na^+ contained in the solid phase prevents its entry into groundwater and promotes a less aggressive geochemical environment in the upper basin than in the lower basin. Consequently, the removal of As and other ions from the mineral carriers is more attenuated in the upper basin than in the discharge zones of the middle–lower basin, which is reflected in the higher As levels in the aqueous phase of the phreatic aquifer.

3.6.3. As and other trace elements (B, F and V) in groundwater: Principal Component Analysis

The phreatic layer morphology has a depth of 1.4 m at the valley bottom and in areas adjacent to the river course, being 41 m in the interfluves towards the southeast. It has a significant hydraulic gradient (6.06‰) and a marked parallelism clearly oriented to the discharge area in Paso de las Piedras Dam (Espósito et al., 2010). Almost all the water samples had excessive As surpassing the reference value in the range of 10 μg L^{-1} to 110 μg L^{-1} and coexisting with other harmful trace elements such as B (120–1420 μg L^{-1}), F (200–4880 μg L^{-1}) and V (40–800 μg L^{-1}) (Table 6). Although excessive As values were determined in the whole basin, the highest excess, indicative of water quality deterioration, were found in the areas of the middle–lower basin. The geographical intrabasin distribution of As in the aqueous phase is irregular; however, the risk increases in the general flow towards the south and extends towards the southeast with more elevated concentrations adjacent to the aquifer discharge and to the river mouth in the dam (Espósito et al., 2010). The analysis of the first two principal components (PC1 and PC2) performed for As, B, F and V explains 87.2% of the total variability in the groundwater resources. Eigenvalues were: 1 (0.69), 2 (0.18) and 3 (0.08). These four main studied variables contribute to the formation of PC1 (Table 9) with a percentage of reconstruction >50% and demonstrate a remarkable hydrochemical heterogeneity of the hydric resources.

The PC1–PC2 biplot (Fig. 5) shows that waters with a better relative quality, owing to lower concentrations of the studied elements, belong to the upper basin, to part of the middle basin and solely to small areas of the lower basin. According to the PC1–PC2 plane waters with more elevated concentrations associated with the middle and lower basin are grouped in the quadrants I and IV. Although excessive As values were determined for the entire basin, the more toxic areas by an association of As-V are grouped in the quadrant IV and belong to the middle–lower basin. In addition, it is worth mentioning that better

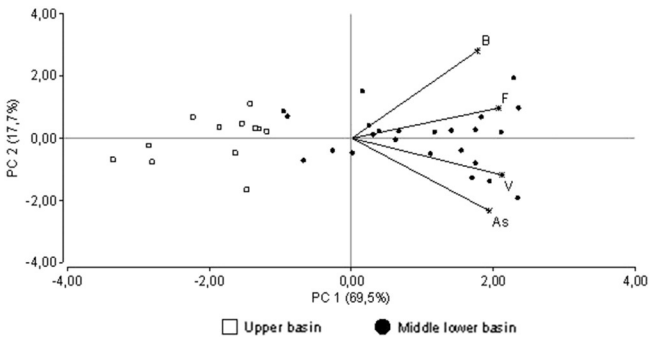

Fig. 5. Biplot PC1–PC2 in groundwaters.

quality waters are located in the sector of the phreatic aquifer that is linked to the upper basin landscape (quadrants II and III).

High pH ranging from near 7 to >9 promotes dissolution of volcanic glass and other As carriers, which cause the formation of As oxyanion species and leaching in loess materials under oxidizing conditions, all them controlled by silicate hydrolysis and carbonate equilibria. Together with Na^+ release from the crystalline structure, calcite dissolution is an important process that brings about high pH values due to CO_2 consumption (Nicolli et al., 2012) in a geochemical environment prone to desorption of As from charged clays. As and other oxyanions of trace elements are adsorbed onto the Al–Fe–Mn oxides and hydroxides of the fine fraction but, when pH increases, they pass to groundwater by desorption, increasing their concentrations up to unacceptable levels. Desorption, enhanced by competition with other oxyions, is a key process for mobility and concentration of As and other trace elements in the phreatic aquifers and evaporation also contributes to the increase of As concentrations in groundwaters.

Moreover, the time–space variability of the As ion concentrations and the associated toxicity is consistent with a more extended residence time of alkaline waters in contact with the aquifer lithology and the subsequent development of weathering reactions favoured by pHs varying from neutral to >9 in Na-bicarbonate type waters.

4. Conclusions

The following conclusions emerge from this study focused on As geoavailability in loess soils–sediments and water quality:

- Zones with As >10 μg L^{-1} in waters imply a health risk for the rural, periurban and, even, urban population who do not have access to tap water. Despite the fact that cases of hydroarsenicism (i.e., severe palmo-plantar lession) were not detected in the studied area, the geochemical characteristics of the environmental matrices, such as loess soils (Holocene) and lithology of loess aquifers (pre-Holocene) containing alkaline sodium-bicarbonated groundwaters, pose a potential danger for health as a result of the exploitation of the shallow aquifers with As above the critical value for human consumption. Future agricultural production planning should also consider this situation since As transference to food (cattle raised and crops irrigated with high As waters) could lead to economical losses.
- Areas at risk extend over zones with As geoavailability levels that do not indicate contamination. The values found are background levels. The geopedogenetic complexity governs lateral and vertical variability of As and other associated elements in the solid phase, yielding a major concentration of As-bearers towards the lower basin.
- Post-sedimentary pedogenesis modifies downward the intraprofile distribution of As, particularly in soils affected by calcification at the base or by clay illuviation. In the upper basin, a greater mineral stability and a less aggressive geochemistry prevent large amounts of As and other associated elements from entering into the solution.
- Mineral dissolution, silicate hydrolysis, oxido-reduction and sorption–desorption onto fine charged particles source As to the soluble phase and regulate its concentration in the flow direction up to >10 μg L^{-1} towards the aquifer's discharge in the middle–lower basin, particularly in the southeast zones.
- Fe_{total} and Fe_{ox} were found in a higher content towards the lower basin owing to sedimentation (Fe_{total}) and weathering and subsequent oxidation (Fe_{ox}).
- Local variability of factors such as soil climate, texture and permeability, landform configuration and slope and a longer residence time of water in contact with the aquifer's lithology plays a role in the intrabasin spatial distribution of As and associated trace elements.
- In the alkaline environments of the middle–lower basin, desorption from surfaces of very fine Fe oxides and charged clays causes As accumulation to be above the critical limit. Moreover, evaporation

of the shallow aquifers also leads to unacceptable levels of As concentrations.

These results are consistent with previous studies carried out by our research group and those developed by other authors. The potential risk of HACRE pathologies in a region where the rural population consumes waters with As levels 2 to 5 times above the WHO recommendations is sufficient grounds for future research aimed at exploring the epidemiology of this disease in this area and making speciation analyses and studies on procedures to lower As to acceptable levels or total removal it from waters at a low cost, thus providing a solution for rural, periurban and urban householders devoid of a public network of potable water.

Acknowledgements

The authors thank the Agencia Nacional para la Promoción Científica y Técnica (ANPCYT, PICT 2012-N°2947), the Consejo Nacional de Investigaciones Científicas y Técnicas (CONICET, PIP 2012-2014 GI) and the Secretaría de Ciencia y Tecnología (UNS, PGI 24/A178) for their grants to develop this research and also the anonymous reviewers who greatly contributed to improve our manuscript with their careful and critical reading and their comments and suggestions.

References

Alexandratos, V., Elzinga, E., Reeder, R., 2007. Arsenate uptake by calcite: macroscopic and spectroscopic characterization of adsorption and incorporation mechanisms. Geochim. Cosmochim. Acta 71 (17), 4172–4187.

Amiotti, N., Blanco, M. del C., Sánchez, L.F., 2001. Complex pedogenesis related to differential Aeolian sedimentation in microenvironments of the Argentine semiarid region. Catena 43, 137–156.

Anawar, H.M., Komaki, K., Akai, J., Takada, J., Ishizuka, T., Takahashi, T., Yoshioka, T., Kato, K., 2002. Diagenetic control on arsenic portioning in sediments of the Bengal River Delta, Bangladesh. Environ. Geol. 41 (7), 816–825.

Besuschio, S.C., Desanzo, A.C., Pérez, A., Croci, M., 1980. Epidemiological association between arsenic and cancer in Argentina. Biol. Trace Elem. Res. (1), 41–55.

Blanco, M. del C., Sánchez, L.F., 1994. Mineralogía de arenas en suelos loessicos del sudoeste pampeano, Argentina. Turrialba 44, 147–159.

Blanco, M. del C., Sánchez, L.F., Vera, M., Aguilar Ruiz, J., 1997. Mineralogía y micromorfología de suelos loessicos con desarrollo moderado en la Llanura Subventánica Occidental Bonaerense, Argentina. Edafología. Rev. Soc. Española de la Ciencia del Suelo 2, 215–219.

Blanco, M. del C., Paoloni, J.D., Morrás, H., Fiorentino, C.E., Sequeira, M.E., 2006. Content and distribution of arsenic in soils, sediments and groundwater environments of the Southern Pampa region, Argentina. J. Environ. Toxicol. 21, 561–574.

Blanco, M. del C., Paoloni, J.D., Morrás, H., Sequeira, M.E., Amiotti, N., Bravo, O., Díaz, S., Espósito, M., 2011. Partition of arsenic in soils, sediments and the origin of naturally elevated concentration in groundwater of the southern Pampa region (Argentina). J. Environ. Earth Sci. 66, 2075–2084.

Blanco, M. del C., Espósito, M., Paoloni, J.D., Sequeira, M.E., Nicolli, H.B., Amiotti, N.M., 2012. Arsénico y otros oligoelementos en los recursos hídricos de la región Pampeana Sur (Argentina): Análisis de los acuíferos freático y termal profundo en el área de Bahía Blanca. Argentina y Ambiente 2012 — I Congreso Internacional de Ciencia y Tecnología Ambiental. (Mar del Plata), pp. 1010–1015.

Bray, R.H., Kurtz, L.T., 1945. Determination of total, organic, and available forms of phosphorus in soils. Soil Sci. 59, 39–45.

Bundschuh, J., Pérez Carrera, A., Litter, M., 2008a. Cap 1.—Introducción: Distribución del arsénico en las regiones Ibérica e Iberoamericana. In: RED IBEROARSEN (Ed.), Distribución del As en las regiones Ibérica e Iberoamericana.

Bundschuh, J., Nicolli, H., Blanco, M. del C., others, 2008b. Cap. 7.—Distribución de arsénico en la región sudamericana. In: RED IBEROARSEN (Ed.), Distribución del As en las regiones Ibérica e Iberoamericana.

CAA (Código Alimentario Argentino; Argentinian Food Code), 1994,. Calidad de aguas de bebida. Cap. E-243, DNPH, Buenos Aires, Argentina.

Chakraborti, D., Rahman, M.M., Das, B., Murrill, M., Dey, S., Mukherjee, S.C., Dhar, R.K., Biswas, K.R., Chowdhury, U.K., Roy, S., Sorif, S., Selim, M., Rahman, M., 2010. Status of groundwater arsenic contamination in Bangladesh: a 14-year study report. Water Res. 44 (19), 5789–5802.

Chatterjee, A., Mukherjee, A., 1999. Hydrogeological investigation of groundwater arsenic contamination in South Calcutta. Sci. Total Environ. 225 (3), 249–262.

Chatterjee, D., Dipti, H., Santanu, M., Ashis, B., Bibhash, N., Bhattacharya, P., Bhowmick, S., Mukherjee-Goswami, A., Saha, D., Hazra, R., Maity, P.B., Mukherjee, A., Bundschuh, J., 2010. Assessment of arsenic exposure from groundwater and rice in Bengal Delta Region, West Bengal, India. Water Res. 44, 5803–5812.

Di Rienzo, J.A., Casanoves, F., Balzarini, M.G., González, L., Tablada, M., Robledo, C.W., 2013. InfoStat. Grupo InfoStat, FCA, Universidad Nacional de Córdoba, Argentina (URL http://www.infostat.com.ar).

Espósito, M.E., Sequeira, M.E., Paoloni, J.D., Amiotti, N.M., 2008. Análisis morfométrico de la cuenca endorreica de El Divisorio, Sudoeste de la Provincia de Buenos Aires: V Jorn. Inter. del Sudoeste Bonaerense: Ambiente y recursos naturales del sudoeste bonaerense: Producción, contaminación y conservación. August 20-22, Bahía Blanca (Argentina).

Espósito, M., Paoloni, J.D., Sequeira, M.E., Amiotti, N.M., Blanco, M. del C., 2010. Natural contaminants (As, B, F and V) in the El Divisorio brook basin, tributary of Paso de las Piedras reservoir source of water provision to urban centers at the southern Pampa plains, Argentina. J. Environ. Prot. 2, 97–108.

Espósito, M., Paoloni, J.D., Sequeira, M., Amiotti, N., Blanco, M. del C., 2011. Natural contaminants in drinking waters (Arsenic, Boron, Fluorine and Vanadium) in the southern Pampean plain, Argentina. J. Environ. Prot. 2, 97–108 (Published online (http:www.Sci Rp.org/journal/jep)).

Fitz, W., Wentzel, W., 2006. Sequestration of arsenic by plants. In: Naidu, R., Smith, E., Owens, G., Bhattacharya, P., Nadebaum, P. (Eds.), Managing Arsenic in the Environment, from Soil to Human Health. CSIRO Publishing, pp. 209–222.

Gaiero, D., Depetris, P., Probst, J.L., Bidart, S., Leleyter, L., 2004. The signature of river- and wind-borne materials exported from Patagonia to the southern latitudes: a view from REEs and implications for paleoclimatic interpretations. Earth Planet. Sci. Lett. 219, 357–376.

Garnier, J.M., Travassac, F., Lenoble, V., Rose, J., Zheng, Y., Hossain, M.S., Chowdhury, S.H., Biswas, A.K., Ahmed, K.M., Cheng, Z., van Geen, A., 2010. Temporal variations in arsenic uptake by rice plants in Bangladesh: the role of iron plaque in paddy fields irrigated with groundwater. Sci. Total Environ. 408, 4185–4193.

Garnier, J.M., Hurel, C., Garnier, J., Lenoble, V., Garnier, C., Ahmed, K.M., Rose, J., 2011. Strong chemical evidence for high Fe (II)-colloids and low As-bearing colloids (200 nm–10 kDa) contents in groundwater and flooded paddy fields in Bangladesh: a size fractionation approach. Appl. Geochem. 26, 1665–1672.

González Uriarte, M., 1984. Geomorfología de la porción continental que rodea a la Bahía Blanca. Proceedings X Congr. Geológico Argentino, S.C. de Bariloche, Argentina vol. III, pp. 556–576.

Halicz, L., Russell, G.M., 1986. Simultaneous determination by hydride generation and induced couple plasma atomic emission spectrometry of arsenic, antimony, selenium and tellurium in silicate rocks containing the noble metals and in sulphide ores. Analyst 111, 15–18.

Hopenhayn-Rich, C., Biggs, M.L., Bergoglio, R., Tello, E., Nicolli, H., Smith, A.H., 1996. Blader cancer mortality associated with arsenic in drinking water in Córdoba, Argentina. Epidemiology 7, 117–124.

Hopenhayn-Rich, C., Biggs, M.L., Smith, A.H., 1997. Lung and kidney cancer mortality associated with arsenic in drinking water in Córdoba, Argentina. Int. J. Epidemiol. 27 (4), 561–569.

Mc Arthur, J.M., Ravenscroft, P., Safiulla, S., Thirwall, M.F., 2001. Arsenic in groundwater: testing pollution mechanisms for sedimentary aquifers in Bangladesh. Water Resour. Res. 37, 109–117.

Mehra, O.P., Jackson, M.L., 1960. Iron oxide removal from soils and clays by a dithionite–citrate system buffered with sodium bicarbonate. Clay Clay Miner. 7, 317–327.

Morrás, H.J., Blanco, M. del C., Paoloni, J.D., 2002. Algunas observaciones sobre el origen del arsénico en sedimentos, suelos y aguas de la región Chaco- Pampeana, Argentina. In: Asoc. Arg. Sedimentology (Ed.), II Taller Sedim y Medio Amb, Buenos Aires, Argentina (November 28–30, Resúmenes, 37–38).

Mukherjee, A., von Brömssen, M., Scanlon, B.R., Bhattacharya, P., Fryar, A.E., Aziz, M., H., Ahmed, K.M., Chatterjee, D., Jacks, G., Sracek, O., 2008. Hydrogeochemical comparison and effects of overlapping redox zones on groundwater arsenic near the western (Bhagirathi sub-basin, India) and Eastern (Meghna sub-basin, Bangladesh) margins of the Bengal Basin. J. Contam. Hydrol. 99, 31–48.

Mukherjee, A., Fryar, A.E., Thomas, W.A., 2009. Geologic, geomorphic and hydrologic framework and evolution of the Bengal basin, India and Bangladesh. J. Asian Earth Sci. 34 (3), 227–244.

Nicolli, H.B., Suriano, J.M., Peral, M.A., Ferpozzi, L.H., Baleani, O.A., 1989. Groundwater contamination with arsenic and other trace elements in an area of the Pampa, province of Cordoba, Argentina. Environ. Geol. Water Sci. 14 (1), 3–16.

Nicolli, H., Smedley, P., Tullio, J., 1997. Aguas subterráneas con alto contenido de flúor, arsénico y otros oligoelementos en el Norte de la provincia de La Pampa: Estudio preliminar. Cong Int sobre Aguas (Workshop on Environmental Chemistry and Health), Buenos Aires, Argentina, August 4–8. Proceedings III-40.

Nicolli, H.B., Blanco, M. del C., Paoloni, J.D., Fiorentino, C.E., 2008. Capítulo 4: Ambientes afectados por el arsénico. In: Bundusch, J., Perez Carrera, A., Litter, M.I. (Eds.), Distribución del arsénico en las regiones Ibérica e Iberoamericana, CYTED-REDIBEROARSEN, pp. 49–76.

Nicolli, H.B., Bundschuh, J., Blanco, M. del C., Tujchneider, O., Panarello, H., Dapeña, C., Rusansky, J., 2012. Arsenic and associated trace elements in groundwater from the Chaco-Pampean plain, Argentina: results from 100 years of research. Sci. Total Environ. 429 (1), 36–56.

Paoloni, J.D., Vázquez, R., Fiorentino, C.E., 1988. La topografía y la variación de las precipitaciones y los escurrimientos en el Sistema de Ventania. Seg. Jorn. Geol.Bonaerenses, Bahía Blanca. Proceedings, pp. 651–661.

Rankama, K., Sahama, T.G., 1962. Geoquímica. Ediciones Aguilar SA. Seg. edición. (Madrid, España, 250 pp.).

Roca, N., Pazos, S., Bech, J., 2012. Background levels of potentially toxic elements in soils: a case study in Catamarca (a semiarid region in Argentina). Catena 92, 55–66.

Smedley, P.L., Kinniburgh, D.G., 2002. A review of the source, behavior and distribution of arsenic in natural waters. Appl. Geochem. 17 (5), 517–568.

Soil Survey Staff, 2006. Soil Survey Manual. Agricultural Research Administration-USDA, Washington, DC, USA (503 pp.).

Soil Survey Staff, 2014. Keys to Soil Taxonomy. Twelfth ed. United States Department of Agriculture, Natural Resources Conservation Service (359 pp.).

USEPA. (U.S Enviromental Protection Agency), 2014. (http://water.epa.gov. date of consultation: Julio 15th, 2015).

USEPA. (U.S Environmental Protection Agency), 2012. Drinking Water Standards and Health Advisories (EPA 822-S-12-001), Washington, DC (20 pp.).
WHO, 2008. Guidelines for drinking-water quality third edition incorporating the first and second addenda. Recommendations vol. 1. World Health Organization, Geneva (668 pp.).
WHO, 2015. Guidelines for drinking-water quality. fourth ed. World Health Edition, Malta (518 pp.).
Xie, Z.M., Naidu, R., 2006. Factors influencing bioavailability of arsenic to crops. In: Naidu, R., Smith, E., Owens, G., Bhattacharya, P., Nadebaum, P. (Eds.), Managing Arsenic in the Environment, from Soil to Human Health. CSIRO Publishing, pp. 223–234.
Zárate, M., 2003. Loess of the southern South América. Quat. Sci. Rev. 22, 1987–2006.
Zárate, M., Tripaldi, A., 2012. The Aeolian system of central Argentina. Aeolian Res. 3, 401–417.